Hindawi Publishing Corporation
Journal of Nanomaterials
Volume 2016, Article ID 6050731, 5 pages
http://dx.doi.org/10.1155/2016/6050731

Research Article

Tin Dioxide Nanocrystals as an Effective Sensitizer for Erbium Ions in Er-Doped SnO_2 Systems for Photonic Applications

Tran T. T. Van,[1] Nguyen Truc Ly,[2] Le T. T. Giang,[1] and Cao Thi My Dung[1]

[1] *University of Science, Vietnam National University Ho Chi Minh City, 227 Nguyen Van Cu Street, Ward 4, District 5, Ho Chi Minh City, Vietnam*
[2] *Ho Chi Minh City University of Technical Education, 1 Vo Van Ngan Street, Linh Chieu Ward, Thu Duc District, Ho Chi Minh City, Vietnam*

Correspondence should be addressed to Tran T. T. Van; tttvan@hcmus.edu.vn

Received 27 June 2016; Accepted 24 August 2016

Academic Editor: Jean M. Greneche

Undoped SnO_2 and erbium-doped SnO_2 powders were successfully prepared by precipitation method. The effect of the heat treatment and doping contents on the structure of tin oxide and optical properties was also studied. The XRD data and Raman spectra indicate that the SnO_2 crystals have formed after being heat-treated at 400°C and the average size of grains is about 8 nm for doping content of 1 mol%. An increase of doping concentration has controlled the growth of nanocrystals. The principle of the visible and infrared emissions of SnO_2 and SnO_2:Er is also discussed. All photoluminescence study shows that the Er^{3+} ions can be located in SnO_2 nanocrystals and that there is energy transfer from defect levels of SnO_2 nanoparticles to neighboring Er^{3+} ions of crystals.

1. Introduction

Erbium-doped semiconductors are considered to be promising optical materials for optoelectronic devices because the emission at 1.54 μm of the Er^{3+} intra-4f shell transition coincides the minimum absorption and dispersion in optical fibers. The incorporation of Er^{3+} ions in nanocrystals not only prevents the aggregation even at high concentrations but also allows the crystal-ion energy transfer, thus enhancing the efficiency of ion luminescence. The energy transfer from semiconductor nanocrystals to Er^{3+} ions can efficiently compensate the small cross-section of rare earth transitions. Numerous works have reported the photoluminescent properties of Er^{3+} ions in different semiconductors host via indirect or direct excitation [1–8].

Tin oxide (SnO_2) is well-known as an n-type semiconductor with a wide band gap (E_g = 3.6 eV at 300 K) and a good host material for rare earth (RE) ions due to its outstanding chemical, optical, electrical, and morphological properties. Moreover, with its very low cutoff phonon energy of 630 cm^{-1}, SnO_2 is prone to reducing the nonradiative decay of multiphonon relaxation of RE ion excited states. Tin oxide nanocrystals can be excited by a broad range of UV radiation wavelengths, as compared to the narrow excitation peaks of the Er^{3+} ions. Therefore, these nanocrystals can be easily and efficiently excited by broadband arc lamps with UV emission and then they transfer energy to the Er^{3+} ions.

The aim of our work is focused on optimizing synthesis parameters such as annealing temperature and erbium concentration in order to achieve maximum luminescence of erbium ions in both visible and infrared regions. In this study, emission spectra show more information about the exact location of Er^{3+} as well as an evidence of efficient energy transfer from SnO_2 nanocrystals to erbium ions.

2. Experimental Technique

In order to prepare the undoped and Er^{3+}-doped SnO_2 nanoparticles, 2 g of tin chloride was dissolved in 4 mL ethanol and stirred for 15 minutes. In the latter case, an amount of erbium nitrate ($Er(NO_3)_3{\cdot}5H_2O$) was dissolved in ethanol and mixed with the solution of tin and stirred for

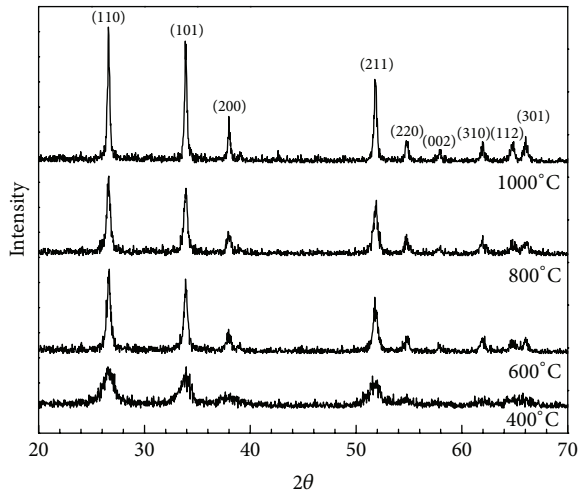

Figure 1: XRD patterns of SnO_2 doped 1% Er^{3+} annealed at different annealing temperatures.

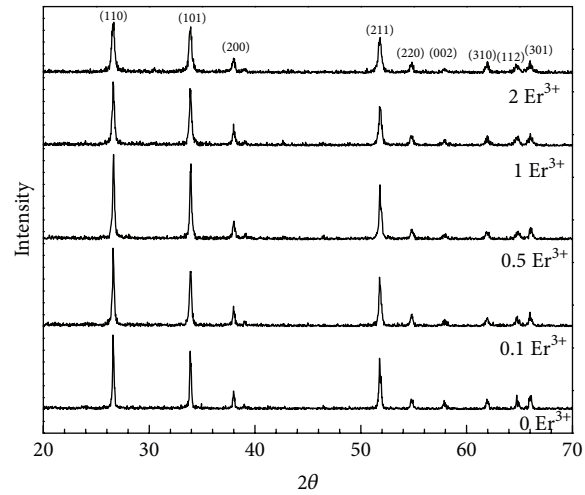

Figure 2: XRD patterns of different Er^{3+} concentrations annealed at 1000°C.

two hours. Aqueous ammonia solution was added dropwise to the above solution and continuously stirred for 30 minutes to form the white precipitates following the reaction:

$$SnCl_2 + 2NH_4OH \longrightarrow Sn(OH)_2 + 2NH_4Cl. \quad (1)$$

These precipitates were filtered and then washed with water and ethanol prior to drying at 55°C for 36 hours. The final powders (SnO_2 and Er^{3+}-doped SnO_2) were calcined at different temperatures ranging from 400°C to 1000°C for 1 hour.

The phases of the samples have been identified by using Bruker D8 diffractometer. The morphology and crystalline size of SnO_2 particles have been determined by transmission electron microscopy (TEM). Fourier transform infrared (FTIR) spectroscopy has been performed in the range of 400–4000 cm^{-1}. The Raman spectra have been obtained using Renishaw InVia Raman Microscope system with a 632 nm excitation wavelength at room temperature. Photoluminescence (PL) has been carried out at room temperature using the wavelength of 300 nm from Xenon ion laser as the excitation source with a luminescence HORIBA JOBIN YVON iHR320.

3. Results and Discussions

3.1. Structural Properties

3.1.1. XRD Diffraction. XRD patterns of the 1 mol% Er^{3+}-doped samples heat-treated at 400°C and 1000°C are displayed in Figure 1. The peaks corresponding to tetragonal rutile-type SnO_2 (JCPDS code 41-1445) are observed for sample, heat-treated at 400°C (the bottom pattern). The intensity evolution of diffraction peaks as a function of annealing temperature indicates an increase of crystallization in the sample. In addition to the peaks characterized for SnO_2 rutile phase, no other peaks are observed, which reveals that the dopant is well dispersed in the SnO_2 host.

XRD patterns of samples with different concentrations of Er^{3+} annealed at 1000°C in Figure 2 show a decrease of intensity with the doping contents. This observation implies that the presence of Er^{3+} ions leads to smaller crystal grains. The ionic radius mismatch of Sn and Er is 28%, where 0.72 Å is of Sn and 1.004 Å is of Er. This difference causes the tensile stress into the SnO_2 matrix, restricting the growth of particle size. That is the reason of the decrease of grain boundaries with increasing Er^{3+} ion in host material. The crystallite size has been calculated using the Scherer formula $D = 0.9\lambda/(\beta \cdot \cos\theta)$ where $\lambda = 1.54$ Å for Cu K_α radiation, β is the full width at half-maximum (FWHM), θ is the corresponding Bragg angle, and k is a constant taken to be 0.9.

Calculation from XRD data of powders doped 1 mol% Er shows that the size of crystal increases from 8 nm for samples annealed at 400°C to 34 nm at 1000°C. This behaviour indicates the agglomeration and represents the particle size growth under the influence of sintering. The sintering temperature promotes enlargement of grain boundaries and consequently particle size increases as a function of annealing temperature [2, 9].

The average size as a function of Er concentrations estimated from XRD data is displayed in Figure 3. The crystallite size decreases gradually from ~50 nm for undoped samples to ~25 nm for samples doped with 2 mol% Er^{3+}. The TEM images of 0% and 2% Er performed in the inset of Figure 3 also prove these results.

3.1.2. Vibrational Spectra. Figure 4 shows the FTIR spectra of 1% Er^{3+}-doped SnO_2 powders heat-treated at different temperatures. For the sample annealed at 400°C, the bands at 1637 and 3426 cm^{-1} are associated with the bending and stretching vibrations of OH groups of some residual water in the powder. The intensity decrease of these bands with the annealing temperatures indicates that the O-H groups can be eliminated by a calcination process. The presence of these OH groups has detrimental effects on optical properties; thus

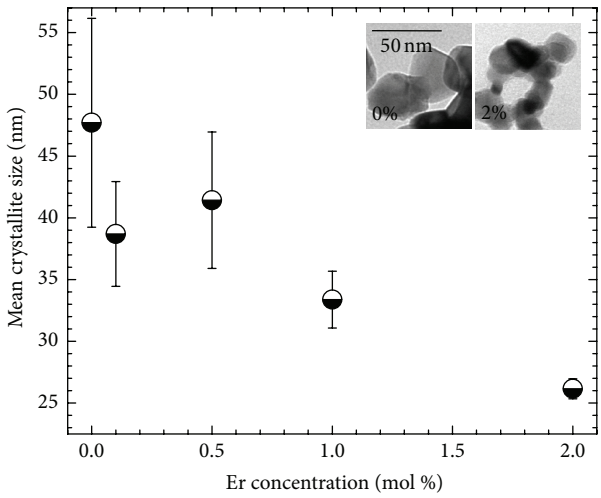

Figure 3: Average size particles of SnO_2 with different Er^{3+} concentrations annealed at 1000°C and insets are TEM images of 0% and 2% Er^{3+}.

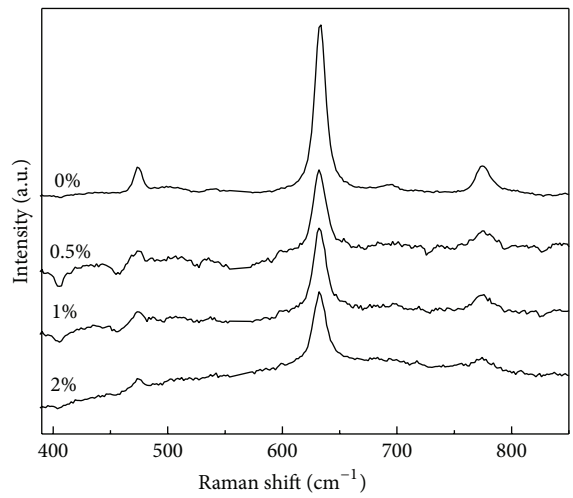

Figure 5: Raman spectra of SnO_2 doped with different Er^{3+} concentrations.

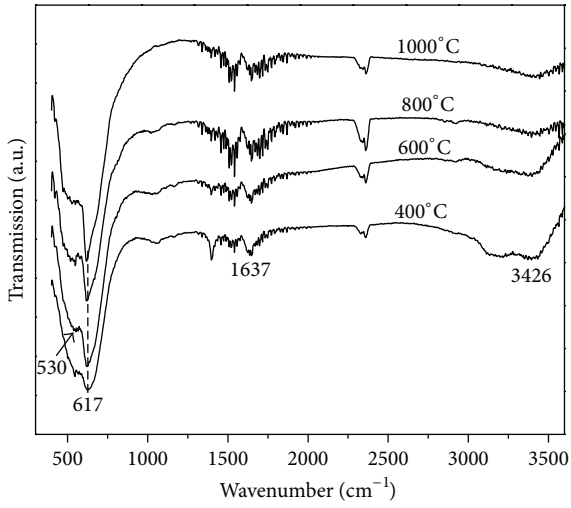

Figure 4: FTIR spectra of 1% Er-doped samples heat-treated at different temperatures.

the samples need to be annealed at temperature as high as 1000°C. The absorption peak at 2352 cm^{-1} is due to O-C-O vibrations of CO_2 modes. The intense peaks at 1403 cm^{-1} are assigned to the typical asymmetrical and symmetrical stretching vibrations of C-O whereas the double weaker peaks located at 1045 cm^{-1} are attributed to the C-O-C symmetrical stretching vibrations [10]. The peak appearing at 617 cm^{-1} is typical of O-Sn-O vibrations of SnO_2, which confirms the presence of SnO_2 as crystalline phase. The band at 530 cm^{-1} is attributed to the terminal oxygen vibration of Sn-OH. These two bands increasing in intensity at higher annealing temperature reflect the growth of nanocrystals. Moreover, the absence of bands related to erbium suggests that these ions were homogeneously dispersed in the host.

The formation of a tetragonal structure of SnO_2 was also depicted via Raman spectra. Figure 5 presents the Raman spectra as a function of Er content in SnO_2 matrix calcined at 1000°C. The three prominent peaks are observed at 473, 633, and 773 cm^{-1} which are characteristic of rutile SnO_2. The scattering peak appearing at 473 cm^{-1} is attributed to the E_g vibrational modes of SnO_2. The highest peak at 633 cm^{-1} corresponds to the A_{1g} symmetric Sn-O stretching mode in nanocrystalline SnO_2 and the peak at 773 cm^{-1} can be assigned to the B_{2g} vibrational modes [7, 11, 12]. The intensity evolution of these modes as a function of annealing temperature shows an increase of the volume of crystals. Another feature to be noted here is the decrease in A_{1g} mode intensity in the Er-doped samples. The reduction of peak intensity suggests that the dopant ions interact strongly with the host, which hinders the crystallization. When the doping concentration increases, the crystallinity decreases. This observation correlates very well with the FTIR, XRD, and TEM data.

3.2. Photoluminescence (PL). The influence of the incorporation of erbium in the tin oxide nanoparticles on luminescence is studied through the photoluminescence measurements of powders with different erbium concentrations. Figure 6 shows the PL spectra under an excitation at 300 nm of SnO_2 powders undoped and doped 0.5%, 1%, and 2 mol% annealed at 1000°C. The spectrum divides into two regimes ranging from visible to IR region.

For the pure SnO_2 sample (the bottom spectrum), a large emission intensity around 620 nm is observed. This band can be attributed to the defect states energy level of SnO_2 nanocrystals. These defect states may originate from oxygen vacancies produced in the annealing process because the organic species would consume oxygen. In the studies of Bonu et al. [13, 14], they have showed that there are two types of "O" vacancies in the SnO_2 crystals which are bridging oxygen (O^B) and in-plane oxygen (O^P) vacancies. Yellow luminescence (YL) (~620 nm) is attributed to the

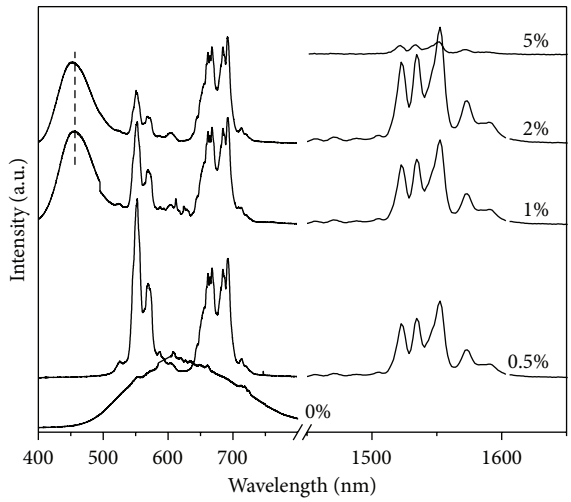

FIGURE 6: PL spectra with different Er^{3+} concentrations under excitation of 300 nm after annealing at 1000°C.

defect states created by O^B vacancies whereas the blue-green luminescence (BGL) is due to O^P vacancies. Thus, it is obvious that the broad emission centred at 620 nm in this case results from O^B vacancies. With the slight erbium doping concentration of 0.5 mol%, we obtain only the narrow characteristic emission peaks at 526 nm, 551 nm, and 665 nm of Er^{3+} ions due to the transition from $^2H_{11/2}$, $^4S_{3/2}$, and $^4F_{9/2}$ level to $^4I_{15/2}$ level, respectively. However, a new emission band at 454 nm appears in the spectra of 1% and 2 mol% Er^{3+}. The substitution of Er^{3+} in Sn^{4+} sites leads to the formation of acceptor states above the valence band of SnO_2 due to the lack of 1-charge. Hence the emission at 454 nm is the result of recombination of electron from conduction band to these acceptor centres. The intensity of this emission increases with doping contents and this band shifts to shorter wavelength due to the fact that an increasing of doping concentration not only induces the more acceptor centres but also shifts the acceptor levels nearer to the valence band [15]. The disappearance of characteristic band at 620 nm of SnO_2 in all spectra of doped samples proves that the energy is efficiently transferred from defect levels of SnO_2 nanocrystals to Er^{3+} ions.

The presence of narrow bands at 1521, 1531, 1549, and 1571 nm in infrared region is assigned to the Stark transitions between $^4I_{13/2}$ and $^4I_{15/2}$ levels of erbium ions. When the erbium ion occupies the Sn^{4+} sites in the cassiterite structure, the electrostatic field of the surrounding environment of ions removes degeneracy of the free ion J levels and makes them split into doubly degenerated Stark levels [16–18]. Upon an indirect excitation at 300 nm, this emission results from energy transfer between SnO_2 nanoparticles and the rare earth ions. The well-resolved sharp Stark-splitting peaks in $^4I_{13/2} \rightarrow {}^4I_{15/2}$ emission in Figure 6 suggest that a significant portion of Er^{3+} ions was incorporated inside a crystalline phase of the host nanoparticles in these Er-doped SnO_2 samples. With increasing erbium concentration, the near-infrared emission intensity at 1540 nm is steadily enhanced. The PL intensity of the 2 mol% Er-doped sample is increased by a factor of about 1.5 compared to that of the 0.5 mol% Er-doped one. However, a noticeable decrease in emission intensity of 5 mol% Er-doped system indicates that quenching of luminescence has occurred with this doping content.

4. Conclusions

In conclusion, Er^{3+}-doped SnO_2 nanoparticles were successfully prepared using the precipitation method with an appropriate heat treatment process. The SnO_2 crystal size increases with annealing temperature and is controlled by doping concentration. A heat treatment at 1000°C is necessary in order to optimize the emission in both visible and infrared regions though the crystal size ranges from 25 nm to 40 nm. The decrease of particle size accompanies the sharp emission peaks of Er^{3+} ions and the appearance of emission at 450 nm indicates that Er^{3+} ions were incorporated in SnO_2 sites. The correlation between luminescence intensity in both visible and infrared regions and doping concentration was demonstrated. All the observations from PL measurements strongly suggest that energy is efficiently transferred from SnO_2 defect levels to the Er^{3+} ions. The emission intensity at 1540 nm is found to be maximum for an Er doping concentration of 2 mol% and then decreases for higher concentrations of Er, which could be attributed to the concentration quenching. The emission at 1540 nm of erbium ions is useful for optical-fiber communication due to the low loss as well as the minimum noise and high gain for this wavelength. The special optical features of these systems make them promising candidates for photonic applications like solar concentrators, green or NIR emitters, and optical amplifiers.

Competing Interests

The authors declare that there is no conflict of interests regarding the publication of this paper.

Acknowledgments

This research is funded by Vietnam National Foundation for Science and Technology Development (NAFOSTED) under Grant no. 103.03-2015.34.

References

[1] Z. Pan, "Photoluminescence of Er-doped ZnO nanoparticle films via direct and indirect excitation," *Journal of Nanophotonics*, vol. 6, no. 1, Article ID 063508, 2012.

[2] R. R. Gonçalves, Y. Messaddeq, M. A. Aegerter, and S. J. L. Ribeiro, "Rare earth doped SnO_2 nanoscaled powders and coatings: enhanced photoluminescence in water and waveguiding properties," *Journal of Nanoscience and Nanotechnology*, vol. 11, no. 3, pp. 2433–2439, 2011.

[3] T. S. Atabaev, "Concentration-dependent optical properties of erbium doped zirconia nanocrystals," *American Journal of Nano Research and Applications*, vol. 2, no. 1, pp. 13–16, 2014.

[4] X. Wang, X. Kong, G. Shan et al., "Luminescence spectroscopy and visible upconversion properties of Er^{3+} in ZnO nanocrystals," *The Journal of Physical Chemistry B*, vol. 108, no. 48, pp. 18408–18413, 2004.

[5] S. Sambasivam, S. B. Kim, J. H. Jeong et al., "Effect of Er^{3+} doping in SnO_2 semiconductor nanoparticles synthesized by solgel technique," *Current Applied Physics*, vol. 10, no. 6, pp. 1383–1386, 2010.

[6] L. P. Ravaro, A. Tabata, J. B. B. Oliveira, and L. V. A. Scalvi, "Raman and photoluminescence of Er^{3+}-doped SnO_2 obtained via the sol-gel technique from solutions with distinct pH," *Optical Materials*, vol. 33, no. 1, pp. 66–70, 2010.

[7] E. A. D. Morais, L. V. A. Scalvi, A. A. Cavalheiro, A. Tabata, and J. B. B. Oliveira, "Rare earth centers properties and electron trapping in SnO_2 thin films produced by sol-gel route," *Journal of Non-Crystalline Solids*, vol. 354, no. 42–44, pp. 4840–4845, 2008.

[8] A. Moadhen, C. Bouzidi, H. Elhouichet, R. Chtourou, and M. Oueslati, "Concentration and temperature dependence of visible up-conversion luminescence in sol-gel SnO_2 doped with erbium," *Optical Materials*, vol. 31, no. 8, pp. 1224–1227, 2009.

[9] A. Gaber, M. A. Abdel- Rahim, A. Y. Abdel-Latief, and M. N. Abdel-Salam, "Influence of calcination temperature on the structure and porosity of nanocrystalline SnO_2 synthesized by a conventional precipitation method," *International Journal of Electrochemical Science*, vol. 9, pp. 81–95, 2014.

[10] H. Chen, L. Ding, W. Sun, Q. Jiang, J. Hu, and J. Li, "Synthesis and characterization of Ni doped SnO_2 microspheres with enhanced visible-light photocatalytic activity," *RSC Advances*, vol. 5, no. 69, pp. 56401–56409, 2015.

[11] L. Tan, L. Wang, and Y. Wang, "Hydrothermal synthesis of SnO_2 nanostructures with different morphologies and their optical properties," *Journal of Nanomaterials*, vol. 2011, Article ID 529874, 10 pages, 2011.

[12] S. K. Pillai, L. M. Sikhwivhilu, and T. K. Hillie, "Synthesis, characterization and photoluminescence properties of Dy^{3+}-doped nano-crystalline SnO_2," *Materials Chemistry and Physics*, vol. 120, no. 2-3, pp. 619–624, 2010.

[13] V. Bonu, A. Das, A. K. Prasad, N. G. Krishna, S. Dhara, and A. K. Tyagi, "Influence of in-plane and bridging oxygen vacancies of SnO_2 nanostructures on CH_4 sensing at low operating temperatures," *Applied Physics Letters*, vol. 105, no. 24, Article ID 243102, 2014.

[14] V. Bonu, A. Das, S. Amirthapandian, S. Dhara, and A. K. Tyagi, "Photoluminescence of oxygen vacancies and hydroxyl group surface functionalized SnO_2 nanoparticles," *Physical Chemistry Chemical Physics*, vol. 17, no. 15, pp. 9794–9801, 2015.

[15] V. Mangalam, K. Pita, and C. Couteau, "Study of energy transfer mechanism from ZnO nanocrystals to Eu^{3+} ions," *Nanoscale Research Letters*, vol. 11, article 73, 2016.

[16] R. Maâlej, M. Dammak, S. Kammoun, and M. Kammoun, "Theoretical investigation of a single erbium center in hexagonal gallium nitride," *Journal of Luminescence*, vol. 126, no. 2, pp. 695–701, 2007.

[17] E. A. Morais, S. J. L. Ribeiro, L. V. A. Scalvi et al., "Optical characteristics of Er^{3+}–Yb^{3+} doped SnO_2 xerogels," *Journal of Alloys and Compounds*, vol. 344, no. 1-2, pp. 217–220, 2002.

[18] X. Wang, X. Kong, Y. Yu, Y. Sun, and H. Zhang, "Effect of annealing on upconversion luminescence of ZnO:Er^{3+} nanocrystals and high thermal sensitivity," *The Journal of Physical Chemistry C*, vol. 111, no. 41, pp. 15119–15124, 2007.